Research Article

Chitin scaffold combined with autologous small nerve repairs sciatic nerve defects

Bo Wang[1, #], Chang-Feng Lu[1, #], Zhong-Yang Liu[2, 3], Shuai Han[1], Pi Wei[1], Dian-Ying Zhang[1], Yu-Hui Kou[1, *], Bao-Guo Jiang[1, *]

Graphical Abstract *A hybird nerve graft composed of chitin scaffords and autologous small nerve was used to repair sciatic nerve defects in rats*
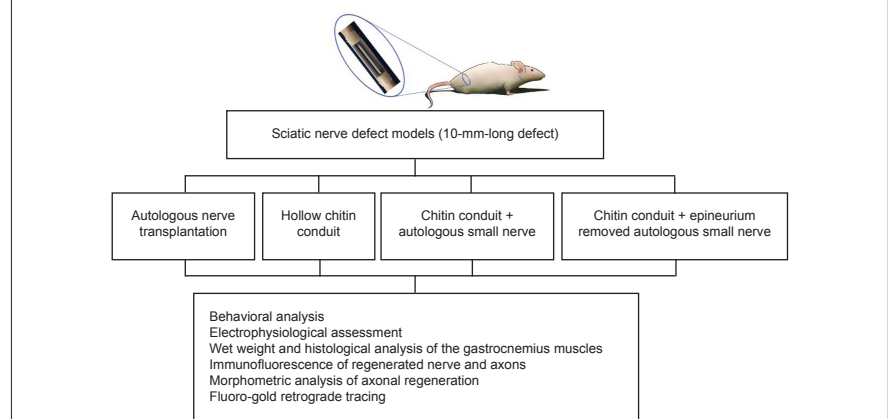
Abstract

Although autologous nerve transplantation is the gold standard for treating peripheral nerve defects, it has many clinical limitations. As an alternative, various tissue-engineered nerve grafts have been developed to substitute for autologous nerves. In this study, a novel nerve graft composed of chitin scaffolds and a small autologous nerve was used to repair sciatic nerve defects in rats. The novel nerve graft greatly facilitated regeneration of the sciatic nerve and myelin sheath, reduced atrophy of the target muscle, and effectively restored neurological function. When the epineurium of the small autogenous nerve was removed, the degree of nerve regeneration was similar to that which occurs after autogenous nerve transplantation. These findings suggest that our novel nerve graft might eventually be a new option for the construction of tissue-engineered nerve scaffolds. The study was approved by the Research Ethics Committee of Peking University People's Hospital (approval No. 2019PHE27) on October 18, 2019.

Key Words: autologous small nerve; chitin scaffold; nerve defect; nervous system; peripheral nerve injury; peripheral nerve regeneration; sciatic nerve; trauma

Chinese Library Classification No. R456; R745; R318.08

Introduction

Peripheral nerve injury remains a major clinical problem, leading to significant patient disability and socioeconomic stress (Noble et al., 1998; Robinson, 2000; Pabari et al., 2011). Nerve defects-gaps in nerves where they have been lesioned-are considered the most serious type of nerve injury. Although the potential for neuronal regeneration in the peripheral nervous system is greater than in the central nervous system, the clinical outcome for nerve defects in the peripheral nervous system is usually incomplete and functional rehabilitation is poor. When a nerve is lesioned, some sort of graft is required to restore the continuity of the nerve and support the growth of nerve fibers. Autologous nerve-graft transplantation is considered the gold standard treatment in these cases (Ray and Mackinnon, 2010) (**Additional Figure 1A and B**). However, its application is limited by the scarce supply of donor nerves, mismatched sizes between the recipient nerve and the donor nerve, and morbidity of the cells around the donor area (Pabari et al., 2011; Maggipinto et al., 2017). As a result, research into alternative treatments, such as tissue-engineered artificial nerves, has been developing rapidly (Jiang et al., 2010; Gu et al., 2014a).

[1]Department of Orthopedics and Trauma, Key Laboratory of Trauma and Neural Regeneration (Ministry of Education/Peking University), Peking University People's Hospital, Beijing, China; [2]Department of Orthopedics, Chinese PLA General Hospital, Beijing, China; [3]National Clinical Research Center for Orthopedics, Sports Medicine & Rehabilitation, Beijing, China
*Correspondence to: Yu-Hui Kou, PhD, yuhuikou@bjmu.edu.cn; Bao-Guo Jiang, MD, PhD, jiangbaoguo@vip.sina.com.
https://orcid.org/0000-0003-1523-825X (Yu-Hui Kou)
#Both authors contributed equally to this work.

Using artificial nerves to bridge gaps within damaged nerves might be able to prevent the invasion of scar tissue and supply a microenvironment that is beneficial for nerve regeneration. Nerve regeneration using a simple, hollow scaffold structure is far from complete because guidance cues and therapeutic factors are lacking (Lu et al., 2018). Numerous efforts have been made to simulate the environment and structure of real autografted nerves in the nerve conduit (Kehoe et al., 2012), such as adding support cells (Gu et al., 2011) and growth factor delivery systems to the conduits (Jiang et al., 2010), and incorporating an array of physical cues to guide the nerve growth (Meyer et al., 2016; Du et al., 2017). However, artificial nerves still cannot be compared with autologous nerve grafts in terms of functional recovery and nerve fiber regeneration (Gu et al., 2014a).

Small noncritical nerves that possess characteristics of autografts have been thought to be able to serve as nerve grafts on the basis of the premise that they can solve the problem of size mismatches (Pan et al., 2020). Indeed, cable-style nerve grafts made from small nerves can match the size of a nerve stump. However, functional recovery is limited by separation of bundles, distortions, and other dysfunction (Daly et al., 2012). Furthermore, to meet the diameter requirement, the length of the small nerve needed to make the cable-style nerve graft is several times that of the defect (**Additional Figure 1C** and **D**). This can lead the single small nerve to become compressed by the surrounding scar tissue. Combining a single autogenous small nerve with artificial nerve scaffolds might provide an enclosed space that allows the damaged nerve to regenerate along the autogenous small nerve. This approach has not been studied in the field of peripheral nerve restoration, and we hypothesized that it might solve the mechanical and size-mismatch problems that accompany the use of a single small nerve. To test this hypothesis, we constructed a chitin scaffold that incorporates a single small autologous nerve with only a few fibers. The length of the small nerve used in this study was the same as the length of the nerve defect. The sources of the small nerve (such as nonessential cutaneous nerves) were more numerous than those for autogenous nerves that matched the size of the injured nerve (**Additional Figure 1E**). The small nerve also provided guiding cues for nerve regeneration, including cells, neurotrophic factors, and oriented, physical guided bridges. The epineurium of the small nerve was removed on the basis of the hypothesis that nerve growth factor could be secreted to the local regeneration environment more efficiently and less scar tissue would form with the removal of fibroblasts. The objective of the study was to investigate the effectiveness of the new nerve graft on peripheral nerve defect repair in a rat model of sciatic nerve defect (10 mm). Because nerve regeneration has been reported to be better in female rats, presumably because female sex hormones have some beneficial effect (Kovacic et al., 2003; Tos et al., 2009; Melcangi et al., 2014), we only selected female rats in this study. This allowed us to rule out the possibility that any differences were due to the sex of the animal. Motor function recovery, axon regeneration, and target muscle reinnervation were evaluated to assess nerve regeneration.

Materials and Methods

Chitin conduit preparation
The chitin conduits have been patented by Peking University People's Hospital and China Textile Academy (Chinese Patent ZL 01136314.2) and were prepared as described previously (Jiang et al., 2006; Rao et al., 2019). Before implantation, all the conduits were sterilized by radiation using 20 kGy ^{60}Co.

Mechanical properties of the chitin conduits
The mechanical properties of the chitin conduits were tested using a universal testing machine (HY-0230; Shanghai Hengyi Instruments Co., Shanghai, China) for biomaterials. The cross-sectional area (S) of the conduit was measured by ImageJ 1.47v (National Institutes of Health, Bethesda, MD, USA) before the test. The two ends of the conduit were fixed in place with a pair of clamps. A pre-load of 1 N was applied to keep the conduit tight and the initial length (L) was measured. Then the sample was stretched at a rate of 10 mm/min. The amount of elongation (ΔL) and the tension (F) were recorded. The amount of elongation at break (ε) was calculated as ε = ΔL/L × 100%, and the tensile strength (σ, MPa) was calculated by the equation: σ = F/S (Wang et al., 2018).

Water penetration and surface characterization of the conduits
A chitin membrane was made by the same technique used to prepare the conduits to evaluate the permeability of water through the wall of the conduit (**Additional Figure 2A**). A valvelike device similar to that reported by Li et al. (2016) was assembled. A layer of filter paper and the chitin membrane was sandwiched between two glass tubes, with the filter paper placed underneath the membrane. Then, 5 mL of crystal violet solution (Sigma-Aldrich (Shanghai) Trading Co. Ltd., Shanghai, China) was added to the upper glass tube (**Additional Figure 2B–D**). After 10 minutes, the device was disassembled and we observed whether the filter paper was stained. The microstructure of the cross-section and the surface of the conduits was observed with a scanning electron microscope (Olympus, Tokyo, Japan).

Animals and surgical operations
All procedures involving animals conformed to the requirements stated in the national standard Laboratory Animals-General for animal experiments (GB/T 35823-2018) and were approved by the Research Ethics Committee of Peking University People's Hospital (approval No. 2019PHE27) on October 18, 2019.

Forty-eight specific pathogen-free (SPF) female adult Sprague-Dawley rats were acquired from Beijing Charles River Laboratories (license No. SCXK (Jing) 2016-0006), aged 8 weeks and weighing 210–240 g. The animals were housed under SPF conditions with temperature controlled between 22–26°C, humidity between 40–70%, and a 12-hour light/dark cycle. The animals were randomly divided into four groups of 12 that received different treatments (see **Table 1** for details): (1) an autograft (Autograft); (2) a hollow chitin biological conduit (C/Hollow); (3) a small autologous nerve (SAN) inside a chitin biological conduit (C/SAN); (4) a small autologous nerve with its epineurium removed (ER) placed inside a chitin biological conduit (C/SAN-ER).

Table 1 | Number of samples in each group of the study

Test item	Autograft group	C/Hollow group	C/SAN group	C/SAN-ER group
Behavioral analysis[*]	6	6	6	6
Electrophysiological tests[*]	6	6	6	6
Weighing and histological analysis of the gastrocnemius muscles[*]	6	6	6	6
Immunofluorescence assay[#]	2	2	2	2
Morphometric analysis of axonal regeneration[*]	6	6	6	6
Fluoro-gold retrograde tracing	6	6	6	6
Total number	12	12	12	12

*The same six rats were used in these tests. #The two samples were randomly chosen from the six rats mentioned above. Autograft group: the nerve gap bridged by the autograft; C/Hollow group: the nerve gap bridged by the hollow chitin conduit; C/SAN group: the nerve gap bridged by the chitin biological conduit in which a small nerve was inside; C/SAN-ER group: the nerve gap bridged by the chitin conduit in which a small nerve with its epineurium removed was inside.

Research Article

All animals were anesthetized via inhalation of 2.5% isoflurane (RWD, Shenzhen, China) using an anesthesia machine for small animals (R500; RWD). Then, the right sciatic nerve was exposed and a segment of the nerve was removed to create a 10-mm-long defect. The resected nerve segment was used to bridge the gap forward by epineural neurorrhaphy in the Autograft group. The gap in the C/Hollow group was bridged with a hollow chitin biological conduit. In the C/SAN group, a small branch of the sciatic nerve from the same animal (10 mm long after retraction) was resected and located in a chitin conduit. The conduit with the nerve was used to bridge the gap. In the C/SAN-ER group, the epineurium of the small branch of the sciatic nerve was stripped before it was placed in the chitin conduit. Otherwise, conditions were the same as in the C/SAN group. The skin was sutured and all rats were housed and fed as usual. The rats were given analgesic jelly after the operation to prevent pain. The animals were carefully observed every day and when signs of autotomy were found, picric acid solution (Sigma-Aldrich (Shanghai) Trading Co. Ltd.) was applied to prevent it from worsening (Firouzi et al., 2015). A schematic diagram of the operation is shown in **Figure 1**.
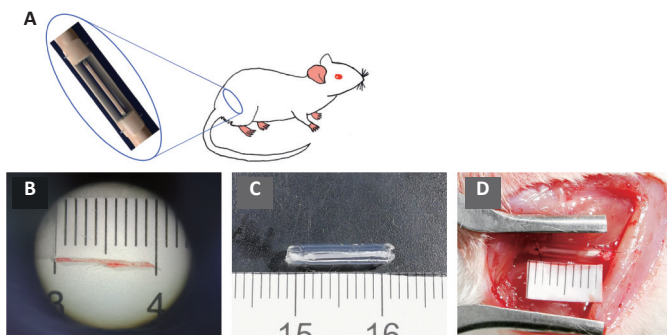
Figure 1 | **The operation procedure.**
(A) A schematic of the operation. (B) Constructing the nerve graft and repairing the sciatic nerve defect. A small branch of sciatic nerve (approximately 1 cm) was used as an autogenous small nerve. (C) The small nerve combined with the chitin conduit. (D) The nerve graft bridging the 10 mm sciatic nerve defect.

Behavioral analysis

Twelve weeks after the operation, motor function recovery was assessed via the Catwalk system (Noldus, Wageningen, the Netherlands) and analyzed by Etho-Vision XT 10.0 software (Noldus). In brief, when placed on an enclosed walkway with a glass floor and black plastic walls, the rats ran all the way to the end where there was a box. The footprints were captured via a high-speed camera placed under the walkway. Footprint intensities were calculated when four paws could be seen in one individual frame. The sciatic function index (SFI) was calculated as below:

SFI = (109.5(eTS − nTS))/nTS − 38.3(ePL − nPL)/nPL + 13.3(eITS − nITS)/nITS − 8.8, in which the print length (PL) is the distance between the heel to the top of the third toe; the toe spread (TS) is the distance from the fifth to the first toe, and the intermediary toe spread (ITS) is the distance from the second to the fourth toe. ePL, eTS, and eITS represent the PL, TS, and ITS for the experimental side (the right hind limb) while nPL, nTS, and nITS were recorded from the normal side (the left hind limb) (Yuan et al., 2020). The values were measured by the Etho-Vision XT 10.0 software. An SFI value of zero suggests normal motor function while a value of −100 indicates full motor dysfunction. The mean intensities (the strength of the footprint) of the left (L, the normal side) and the right (R,

injured side) limbs were measured by the Catwalk system and the R/L ratio was calculated. A higher score means a better motor function outcome (Wang et al., 2020). The tests were carried out by a researcher who was blind to the grouping.

Electrophysiological assessment

Twelve weeks after the operation, electrophysiological tests were carried out before the animals were sacrificed. The repaired sciatic nerve was revealed after anesthesia with 2.5% isoflurane. Stimulating electrodes (Synergy electrophysiology instrument, Oxford, UK) were set at proximal and distal sites of the repaired segment and electrical stimulation (3 mA, 0.1 ms, 1 Hz) was applied. The compound muscle action potentials (CAMPs) of the target gastrocnemius were recorded using an electrode. The peak amplitudes and latencies of the CAMPs were collected for quantitative analysis.

Wet weight and histological analysis of the gastrocnemius muscles

The rats were anesthetized by inhaling 2.5% isoflurane and the gastrocnemius muscles of the right hind limbs and normal left hind limbs were harvested 12 weeks after the operation and weighed immediately using an electronic balance (Lichen, Shanghai, China). The wet weight ratio (right/left) of the muscles was calculated. After the muscles were fixed in 4% (v/v) paraformaldehyde at 4°C for 1 week, 7.0-µm thick transverse sections of the muscles were made and stained via a Masson's Trichrome Stain Kit (G1340, Solarbio, Beijing, China). Briefly, after regular dewaxing, the sections were stained in Weigert ferroxylin solution for 5 minutes. Then, the slides were differentiated with acidic ethanol solution for 5–15 seconds and washed with water. After that, the slides were stained in Masson blue solution for 3–5 minutes, washed with water and distilled water, then stained with magenta solution for 5–10 minutes. After being washed with phosphomolybdate solution for 1–2 minutes and weak acid solution for 1 minute, the slides were dyed in aniline blue solution for 1–2 minutes. Then, the sections were rinsed in weak acid solution for 1 minute, dehydrated, transparentized, and sealed with neutral gum. Five slides were randomly selected from each group and five random fields in each section were chosen for quantitative analysis in which the cross-sectional area of muscle fiber was determined using ImageJ. The average cross-sectional area of the muscle fibers was calculated and compared.

Immunofluorescence and histological assay of regenerated nerve and axons

Twelve weeks after the operation, two rats in each group were randomly chosen and their nerve grafts were harvested. Serial longitudinal sections (10-µm thick) of the grafted segments were prepared on a cryostat (Leica, Weztlar, Germany). After incubation with 10% (v/v) normal goat serum (Sigma-Aldrich (Shanghai) Trading Co. Ltd.) for 10 minutes, the sections were stained with primary rabbit anti-S100 antibodies (Schwann cells marker; 1:200; Cat# S2644, Sigma-Aldrich (Shanghai) Trading Co. Ltd.) and mouse anti-NF200 antibodies (neurofilament marker; 1:400; Cat# N5389, Sigma-Aldrich (Shanghai) Trading Co. Ltd.) at 4°C for 12 hours. Then, the second goat anti-mouse IgG antibodies (Alexa Fluor 488, 1:200, Cat# ab150113, Abcam (Hong Kong), Hong Kong, China) and goat anti-rabbit IgG antibodies (Alexa Fluor 594, 1:200, Cat# ab150084, Abcam (Hong Kong)) were added and the sections were incubated for 1 hour at room temperature. Finally, the sections were incubated with 4′,6-diamidino-2-phenylindole (Abcam (Hong Kong)) for 5 minutes after being rinsed with phosphate buffered saline three times. The stained slides were analyzed with an Axio Scan digital slide scanner (Zeiss,

Oberkochen, Germany) to assess whether the nerve fibers had regenerated through the nerve graft. Hematoxylin-eosin (HE) staining of the longitudinal sections was also performed with an HE staining kit (g1120, Solarbio) and observed with the Axio Scan digital slide scanner to evaluate the inflammatory response.

Morphometric analysis of axonal regeneration

Twelve weeks after the operation, the regenerative nerves 2 mm away from the distal end of the nerve grafts were quickly harvested and fixed in 2.5% (w/v) glutaraldehyde for 2 hours and post-fixed in 1% (w/v) osmium tetroxide for 2 hours at 4°C. After dehydration using series of graded ethanol solutions, the tissues were embedded in Epon 812 epoxy resin (Sigma-Aldrich (Shanghai) Trading Co. Ltd.) and cut into semi-thin (1 μm) and ultrathin (70 nm) sections transversely. The semi-thin sections were dyed with 1% (w/v) toluidine blue and observed under a light microscope (Leica). Five sections were randomly selected from each group and images of five fields in each semi-thin section were randomly chosen to calculate the number of myelinated axons per mm^2. The ultrathin sections were dyed with lead citrate and uranyl acetate and observed with a transmission electron microscope (Olympus). The G-ratio (calculated as the ratio of the inner to outer myelinated axon diameter) and the thickness of myelin sheaths were determined for 80 axons from each animal and at least three animals from each group.

Fluoro-gold retrograde tracing

Retrograde labeling was carried out and back-labeled neurons were counted 12 weeks post-operation. Briefly, the rats were anesthetized by isoflurane and the right sciatic nerve was exposed. Then, the nerve was cut 5 mm away from the distal end of the nerve graft. The proximal end of the severed nerve was immersed in 4% Fluoro-gold (FG; Abcam (Hong Kong)) for 2 hours. Then, the rats were returned to their cages for one week after the incision was sutured. After that, the rats were perfused with 4% paraformaldehyde (w/v) under anesthesia and the lumbar spinal cord (L4–6) and the corresponding dorsal root ganglia were harvested. After fixation in 4% paraformaldehyde for 2 hours and dehydration in 20% sucrose overnight, the samples were cut into frozen sections and observed via a fluorescence microscope (Leica). The numbers of FG labeled motor and sensory neurons were calculated.

Statistical analysis

All the data are expressed as the mean ± standard deviation (SD) and were analyzed with Origin 2019 software (OriginLab, Northampton, MA, USA). One-way analysis of variance (ANOVA) was performed to statistically compare differences between multiple groups. Tests of homogeneity of variances were performed and Student-Newman-Keuls was used with equal variances. $P < 0.05$ was considered statistically significant.

Results

Physical and surface characterization of the chitin conduits

The chitin conduits were generally transparent (**Figure 2A** and **B**). Their elongation at the time of break was 119.45 ± 4.21%, and their tensile strength was 2.34 ± 0.12 MPa (**Figure 2C** and **D**). In the water penetration test, the filter paper under the membrane was dyed purple (**Additional Figure 2E**) and the membrane remained intact without damage (**Additional Figure 2F**), indicating that the crystal violet solution can permeate through the chitin membrane. Scanning electron microscopy pictures of the cross-section and the surface of the conduits showed nanoscale porous structures (**Figure 2E–H**).
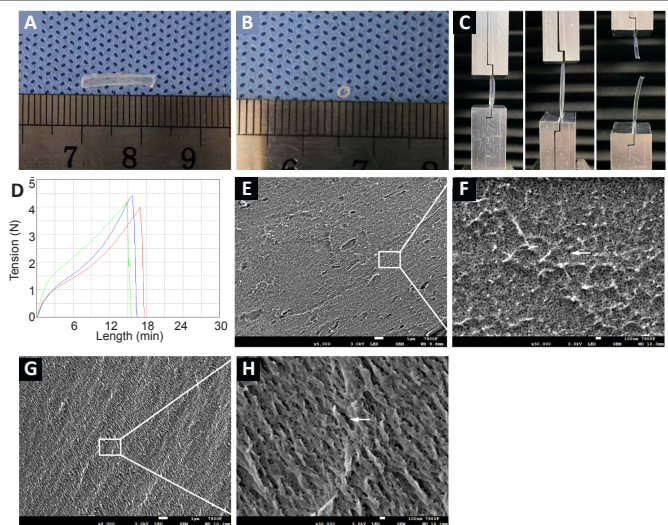
Figure 2 | Appearance and mechanical properties of the chitin conduits.
(A, B) The gross appearance of the chitin conduit. (C) Image showing how the mechanical properties of the chitin conduit were tested. (D) The elongation and the tension of the samples. Three samples were tested and the mean values were calculated. (E–H) The surface (E, F) and cross-section (G, H) of the conduits observed by scanning electron microscope. Arrows indicate the porous structures. Scale bars: 1 μm in E, G; 100 nm in F, H.

Chitin scaffold combined with an autologous small nerve improves motor function recovery in rats with sciatic nerve defects

Twelve weeks after the surgery, gait analysis was carried out to assess motor function recovery. Sciatic nerve injury leads to an increase in footprint length, foot drop, and reduces the distance between toes. Representative footprints graphed by the Catwalk system are shown in **Figure 3A**. The toes on the right side (injured) in autograft and C/SAN and C/SAN-ER groups were more spread out than those in the C/Hollow group. Furthermore, qualitative analysis (**Figure 3B**) showed that SFI values were higher in the C/SAN and C/SAN-ER groups than in the C/Hollow group ($P < 0.01$), while no difference was found between the C/SAN and C/SAN-ER groups ($P = 0.588$). The SFI values in the Autograft group were significantly higher than those in the other groups ($P < 0.01$).

Meanwhile, footprint intensity is qualitative indication of motor function recovery (Sun et al., 2018) (**Figure 3C**). The R/L ratios were higher in the C/SAN and C/SAN-ER groups than in the C/Hollow group ($P < 0.05$), and not different from the Autograft group ($P > 0.05$; **Figure 3D**).

Chitin scaffold combined with an autologous small nerve improves the electrophysiological recovery in rats with sciatic nerve defects

CAMP peak amplitudes and latencies were analyzed as part of the electrophysiological assessment of nerve conduction recovery. The CAMP peak amplitude is related to the number of innervated muscle fibers while the CAMP latency is affected by the thickness of the myelin sheath around the regenerated nerve and the degree of myelination (Lu et al., 2018). Representative CAMP curves from the four groups are shown in **Figure 4A–D**. CAMP amplitudes were significantly higher in the C/SAN and C/SAN-ER groups than in the Hollow group ($P < 0.01$). Moreover, the amplitude in the C/ER-SAN group was higher than that in the C/SAN group ($P < 0.01$) and similar to that of the Autograft group (**Figure 4E**). CAMP latency in the C/ER-SAN group was significantly lower than that in the C/Hollow group ($P < 0.01$) and significantly higher than that in the Autograft group ($P < 0.05$; **Figure 4F**).
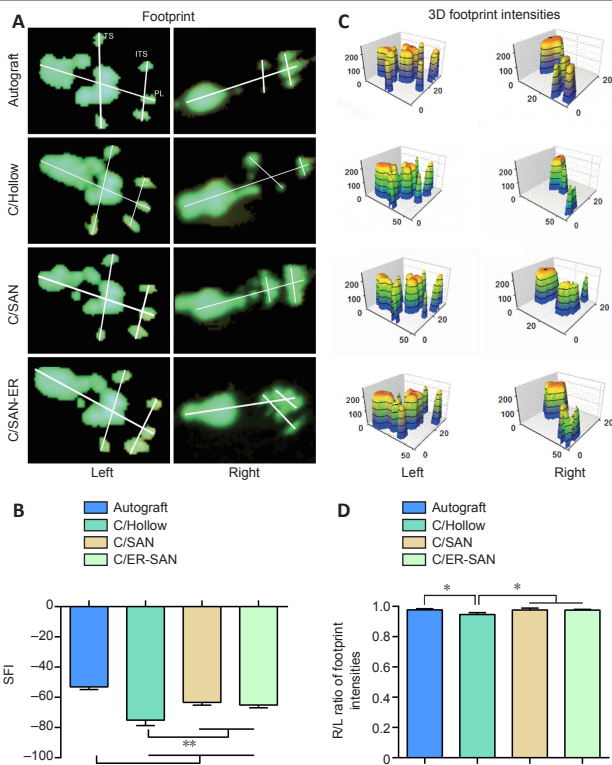
Figure 3 | Chitin scaffold combined with autologous small nerve improves motor function recovery in rats 12 weeks after induction of sciatic nerve defects.

(A) Representative left and right hindfoot footprints in each group. (B) Quantitative SFI values in each group. (C) The 3D footprint intensities of the four groups. The lower the SFI values, the more severe the motor dysfunction. (D) Quantitative results of the R/L ratio of footprint intensities for the four groups. Data are expressed as mean ± SD (n = 6). *P < 0.05, **P < 0.01 (one-way analysis of variance followed by Student-Newman-Keuls test). Autograft group: the nerve gap bridged by the autograft; C/Hollow group: the nerve gap bridged by the hollow chitin conduit; C/SAN group: the nerve gap bridged by the chitin biological conduit in which a small nerve was inside; C/SAN-ER group: the nerve gap bridged by the chitin conduit in which a small nerve with its epineurium removed was inside. 3D: Three dimensions; ITS: intermediary toe spread; L: left; PL: print length; R: right; SFI: sciatic function index; TS: toe spread.
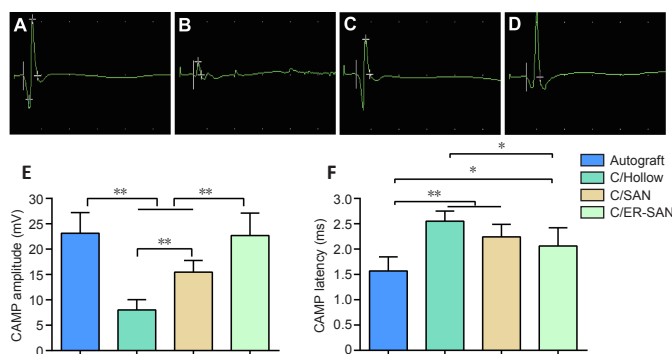
Figure 4 | Chitin scaffold combined with autologous small nerve improves the electrophysiological assessment results in rats 12 weeks after inducing sciatic nerve defects.

(A–D) Representative images of the CAMP for the Autograft (A), C/Hollow (B), C/SAN (C), and C/SAN-ER (D) groups. (E) The mean CAMP amplitude for each group. (F) The mean CAMP latency for each group. Autograft group: the nerve gap bridged by the autograft; C/Hollow group: the nerve gap bridged by the hollow chitin conduit; C/SAN group: the nerve gap bridged by the chitin biological conduit in which a small nerve was inside; C/SAN-ER group: the nerve gap bridged by the chitin conduit in which a small nerve with its epineurium removed was inside. Data are expressed as mean ± SD (n = 6). *P < 0.05, **P < 0.01 (one-way analysis of variance followed by Student-Newman-Keuls test). CAMP: Complex muscle action potential.

Chitin scaffold combined with an autologous small nerve improves the gastrocnemius recovery in rats with sciatic nerve defects

Gastrocnemius atrophy occurs after sciatic nerve transection and stops after reinnervation (Du et al., 2017). The degree of muscle atrophy was assessed 12 weeks after the operation to determine whether the denervated skeletal muscle could be re-innervated. Gross images of the gastrocnemius from both sides are shown in **Figure 5A**. Obviously atrophic muscles were observed in the C/Hollow group while attenuated muscle loss was found in the other groups. The wet weight ratios of the gastrocnemius in the C/SAN and C/SAN-ER groups were significantly higher than those in the C/Hollow group (P < 0.01), while still lower than that in the Autograft group (P < 0.05; **Figure 5B**).

Representative Masson's stained images of muscles in the injured side are displayed in **Figure 5A**. Measurements of the mean cross-sectional area of muscle fibers further confirmed the more satisfying recovery in the C/SAN and C/SAN-ER groups relative to the C/Hollow group (P < 0.01; **Figure 5C**). However, the Autograft group made the best muscle recovery (P < 0.05; **Figure 5B**).

Chitin scaffold combined with an autologous small nerve improves sciatic nerve regeneration and remyelination in rats with sciatic nerve defects

HE and NF200/S100 immunofluorescence stain of the nerve grafts showed that the nerve fibers in all groups successfully regenerated through the nerve graft (**Figure 6**) with no inflammatory cell infiltration. However, double immunofluorescence staining indicated that the morphologic appearance was better in the Autograft, C/SAN, and C/SAN-ER groups than in the C/Hollow group (**Figure 6A3–D3**). Additionally, nerve tissue in the chitin scaffold was more evenly distributed and regeneration was stronger in the C/SAN and C/SAN-ER groups than in the C/Hollow group (**Figure 6B3, C3**, and **D3**).

We quantified the density of regenerated axons by examining the semi-thin sections of regenerated nerve fibers that were dyed with toluidine blue. Axon density was greater in the C/SAN, C/SAN-ER, and Autograft groups than in the C/Hollow group (**Figure 7A–D**). We also quantified the number and density of axons within ultrathin sections that we observed using a transmission electron microscope (**Figure 7E–P**). The Autograft group had the highest number of regenerated axons, and axon density was again shown to be higher in the C/SAN and C/SAN-ER groups than in the C/Hollow group (P < 0.05; **Figure 7Q**).

Myelin sheath thickness, which is an index of nerve maturity (Maggipinto et al., 2017), was significantly greater in the Autograft and C/SAN-ER groups than that in the C/Hollow group (P < 0.01), but not significantly different from each other (P = 0.208; **Figure 7R**). The myelin sheath in the C/SAN group was significantly thicker than that in the C/Hollow group (P < 0.01), but thinner than what we observed in the Autograft and C/SAN-ER groups (P < 0.05; **Figure 7R**). Moreover, G-ratio measurement suggested that remyelination of the regenerated nerve fibers in the Autograft, C/SAN, and C/SAN-ER groups was better than that in the C/Hollow group (P < 0.05; **Figure 7S**).

Retrograde staining of spinal motoneurons and dorsal root ganglia sensory neurons with FG can occur if new axons regenerate through the scaffolds successfully (Zhu et al., 2014). Representative FG labeled neurons are showed in **Figure 8A–H**. The number of stained neurons was similar between the C/SAN-ER and Autograft groups, and was significantly higher in these two groups than in the other groups (P < 0.01). The fewest number of FG labeled neurons was observed in the C/Hollow group (P < 0.01; **Figure 8I** and **J**).
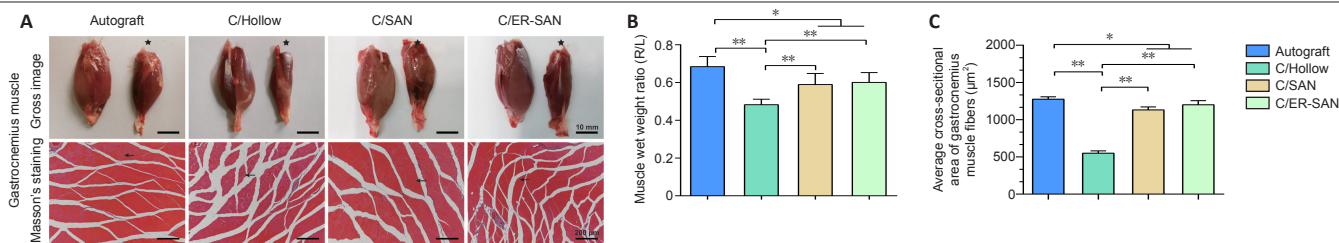
Figure 5 | Chitin scaffold combined with autologous small nerve affects the histology and weight of the gastrocnemius muscle in rats with sciatic nerve defects.

(A) Representative gross images of the gastrocnemius muscle on the normal and surgical side (stars), and images of Masson's trichrome stained transverse sections of the muscles on the surgical side. Arrows indicate the muscle fibers. The muscles in the C/SAN and C/SAN-ER groups were much larger than those in the C/Hollow group. The gap between muscle fibers was larger in the C/Hollow group than in the C/SAN and C/SAN-ER groups. Scale bars: 10 mm (upper), 20 μm (lower). (B) Muscle wet weight ratio for the four groups. (C) Average cross-sectional muscle fiber area for the four groups. Data are expressed as mean ± SD (n = 6). *P < 0.05, **P < 0.01 (one-way analysis of variance followed by Student-Newman-Keuls test). Autograft group: the nerve gap bridged by the autograft; C/Hollow group: the nerve gap bridged by the hollow chitin conduit; C/SAN group: the nerve gap bridged by the chitin biological conduit in which a small nerve was inside; C/SAN-ER group: the nerve gap bridged by the chitin conduit in which a small nerve with its epineurium removed was inside. R/L: Right/left.
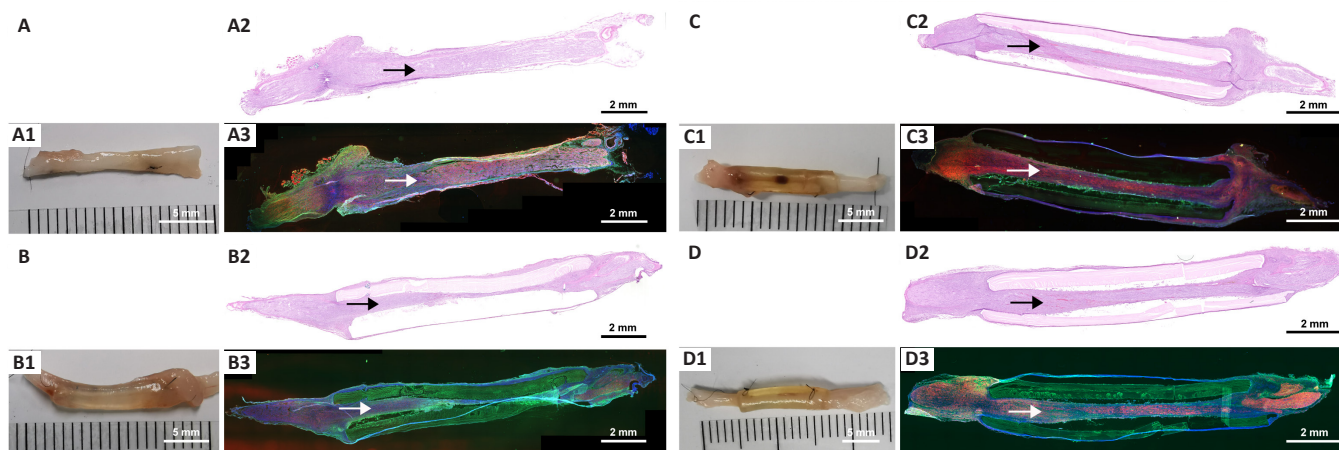
Figure 6 | Chitin scaffold combined with autologous small nerve improves sciatic nerve regeneration in rats wit sciatic nerve defects.

(A–D) HE and double immunofluorescence assay of the nerve graft in Autograft (A), C/Hollow (B), C/SAN (C), and C/SAN-ER (D) groups. (A1–D1) Gross images of the regenerated nerve through the grafts. (A2–D2) HE staining and (A3–D3) double immunofluorescence staining of the nerve grafts (NF200, Alexa Fluor 488, green; S100, Alexa Fluor 594, red; DAPI, blue). Arrows indicate the regenerated nerve fibers through the nerve graft. Compared with the C/Hollow group, the C/SAN and C/SAN-ER groups showed stronger nerve tissues. Scale bars: 5 mm in A1–D1; 2 mm in A2–D2 and A3–D3. Autograft group: the nerve gap bridged by the autograft; C/Hollow group: the nerve gap bridged by the hollow chitin conduit; C/SAN group: the nerve gap bridged by the chitin biological conduit in which a small nerve was inside; C/Hollow group: the nerve gap bridged by the hollow chitin conduit; C/SAN-ER group: the nerve gap bridged by the chitin conduit in which a small nerve with its epineurium removed was inside. DAPI: 4′,6-Diamidino-2-phenylindole; HE: hematoxylin-eosin; NF200: neurofilament 200.
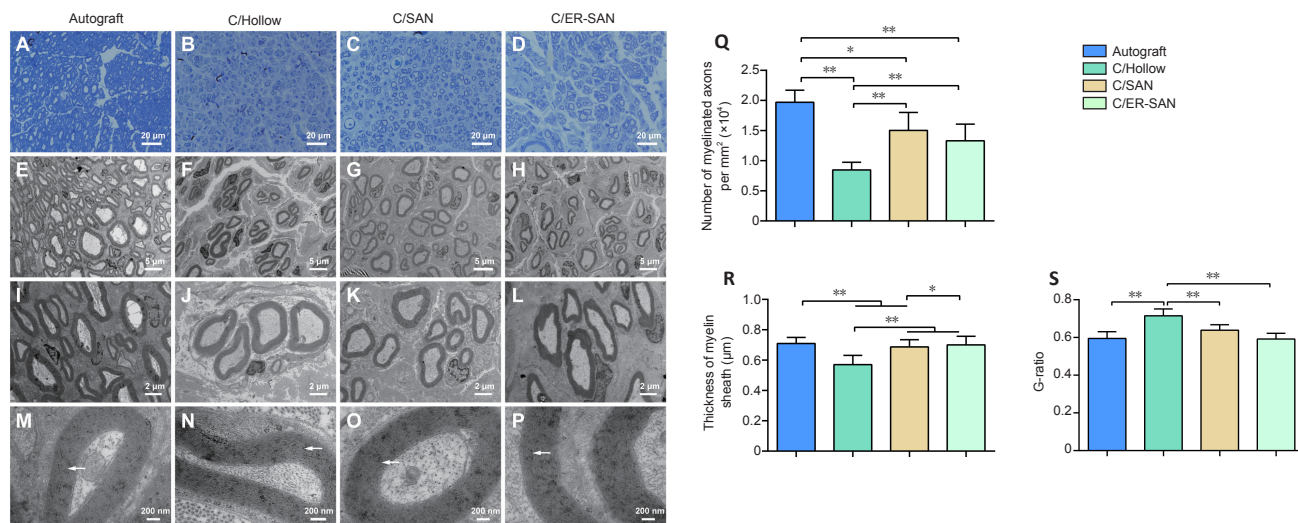
Figure 7 | Chitin scaffold combined with autologous small nerve affects the morphometric parameters of axonal regeneration in rats with sciatic nerve defects.

(A–D) Representative toluidine blue images of regenerated axons in the four groups. Axon density was higher in the C/SAN and C/SAN-ER groups than in the C/Hollow group. (E–P) Representative transmission electron microscopic images of the regenerated axons. The thickness of myelin sheath was greater in the C/SAN and C/ER-SAN groups than in the C/Hollow group. Arrows indicate the structure of the myelin sheath. Scale bars: 20 μm in A–D; 5 μm in E-H; 2 μm in I-L; 200 nm in M–P. (Q) The number of myelinated axons in the four groups. (R) The thickness of the myelin sheath in the regenerated axons. (S) The G-ratios of the myelinated axons in the four groups. Data are expressed as mean ± SD (n = 6). *P < 0.05, **P < 0.01 (one-way analysis of variance followed by Student-Newman-Keuls test). Autograft group: the nerve gap bridged by the autograft; C/Hollow group: the nerve gap bridged by the hollow chitin conduit; C/SAN group: the nerve gap bridged by the chitin biological conduit in which a small nerve was inside; C/SAN-ER group: the nerve gap bridged by the chitin conduit in which a small nerve with its epineurium removed was inside.

Research Article
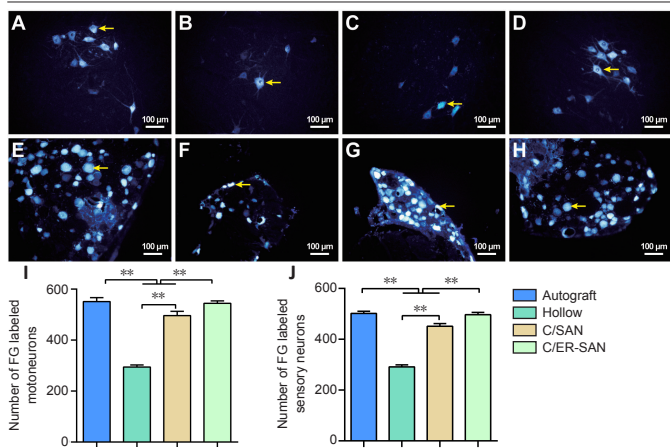
Figure 8 | Fluoro-gold (FG) retrograde labeled motoneurons and sensory neurons in the sciatic nerve of rats with chitin scaffold combined with autologous small nerve treatment.

(A–D) FG labeled motoneurons in the Autograft (A), C/Hollow (B), C/SAN (C), and C/SAN-ER (D) groups. (E–H) FG labeled sensory neurons in the Autograft (E), C/Hollow (F), C/SAN (G), and C/SAN-ER (H) groups. (I, J) The number of FG labeled motoneurons (I) and sensory neurons (J) in 200-fold field of each group. The number of FG labeled motoneurons and sensory neurons was greater in the C/SAN and C/SAN-ER groups than in the C/Hollow group, and greater in the C/SAN-ER group than in the C/SAN group. Arrows indicate the FG labeled neurons. Data are expressed as mean ± SD ($n = 6$). *$P < 0.05$, **$P < 0.01$ (one-way analysis of variance followed by Student-Newman-Keuls test). Autograft group: the nerve gap bridged by the autograft; C/Hollow group: the nerve gap bridged by the hollow chitin conduit; C/SAN group: the nerve gap bridged by the chitin biological conduit in which a small nerve was inside; C/SAN-ER group: the nerve gap bridged by the chitin conduit in which a small nerve with its epineurium removed was inside.

Discussion

Neurotmesis is the most severe peripheral nerve injury according to the classification system in Seddon et al. (1943), and neurotmesis with a gap larger than 5 mm rarely heals with complete axonal regeneration and functional recovery (Cunha et al., 2011). Thus, a nerve graft is required to restore nerve continuity. Developing promising alternatives to autogenous nerve grafts remains a crucial challenge for those in the field of peripheral nerve-defect repair. In the present study, we constructed a nerve graft composed of a small autogenous nerve, with or without its epineurium, inside a chitin conduit. We used a rat model with 10-mm-long sciatic nerve defect, which is a classical, reliable, and widely used model for research in the field of nerve regeneration (Gu et al., 2014b; Das et al., 2015; Lu et al., 2018; Tang et al., 2019). Although 10-mm sciatic nerve gaps exhibit a certain degree of spontaneous nerve regeneration through a hollow graft, functional recovery is usually poor. Additionally, despite some inspiring results, repairing 10-mm sciatic nerve gaps using tissue-engineered nerve grafts has not gone beyond the laboratory stage and cannot replace autologous nerve grafts, which remain the clinical gold standard. In this study, the C/Hollow group, in which the defect was bridged by a hollow chitin conduit, was the negative control, and the Autograft group, in which the gap was repaired by a resected nerve segment, was the positive control. Female rats were selected for constructing the animal models the sex of rats is known to affect the regenerative capabilities of peripheral nerves (Casal et al., 2018); female rats showed better outcome after peripheral nerve injury, perhaps related to their different hormones (Kovacic et al., 2003; Tos et al., 2009; Melcangi et al., 2014). On the basis of this fact, other peripheral nerve-regeneration studies often use female rats to maximize the differences between groups (Tos et al., 2009), which thus allows the ruling out of sex as a reason for any observed differences.

Chitosan is widely used as a biomaterial due to its biocompatibility and biodegradability (Carvalho et al., 2017). Materials made from chitosan have also been studied in the repair of injured nerves (Wang et al., 2005; Gu et al., 2014b; Carvalho et al., 2017). The chitin conduits used in this study were made from partially acetylated chitosan. These chitin conduits have good mechanical properties and have been used with satisfactory outcomes to repair injured nerves in our previous studies (Xue et al., 2015; Zhang et al., 2015; Rao et al., 2019, 2020). In this study, the chitin nerve conduit maintained reliable mechanical support for the combined nerve graft and blocked the infiltration of scar tissue that can hinder axon regeneration. The gross imaging and immunofluorescence staining of the nerve grafts 12 weeks after surgery showed that nerve fibers successfully regenerated through chitin conduits, without any collapse or breakage of the scaffold. The wall of the conduit was permeable to water, which was helpful for the exchange of nutrients. Additionally, neurotrophic factors secreted by the small nerve graft and the injured nerve stump can accumulate in the chitin conduit, creating a favorable niche for nerve growth.

The outcomes of hollow conduits in nerve defect repair are often poor due to the shortage of guidance cues and the non-optimal microenvironment for promoting nerve regeneration (Kehoe et al., 2012). Great efforts have been made to add physical and biological fillers to the hollow conduit to simulate the construction of autogenous nerve, such as chitosan-film (Meyer et al., 2016), aligned fibers (Madduri et al., 2010; Rao et al., 2020), hydrogels (Lu et al., 2018), extracellular matrix (Gu et al., 2014b), neurotrophic factors or functionalized peptides (Lu et al., 2018), and other support cells (Georgiou et al., 2015). The progress is encouraging, and these designs have been able to partially simulate the structure and function of autogenous nerves; however, the therapeutic outcome is still not comparable to that of autogenous nerve transplantation. The natural microenvironment for nerve regeneration is a combination of many factors, rather than a single factor, which promote effective peripheral nerve regeneration. Therefore, the ideal microenvironment for peripheral nerve regeneration should be a biological network containing multiple factors, and to date, using autogenous nerves is the most promising way to for that environment to be constructed. Due to the limited sources of autogenous nerves of appropriate size and length, we chose small autogenous nerves as the core guidance cue, which were easy to get in clinical practice. By placing the small nerve into the chitin conduit, the problem of mismatched size was solved, and the chitin walls provided appropriate mechanical support, as described above. The small nerve graft itself was also an injured nerve that could lead to the proliferation of Schwann cells (SCs) and neurotrophic factor secretion (Zhang et al., 2008). Additionally, the intact small nerve provides a hierarchically aligned structure that is crucial for nerve repair (Cui and Ge, 2007; Pan et al., 2020; Rao et al., 2020).

We investigated the efficacy of the combined graft in repairing rat sciatic nerve defect. Twelve weeks after implantation, the SFI values, CAMP amplitude, and histological analysis of gastrocnemius in the C/SAN and C/ER-SAN groups were all significantly improved over the C/Hollow group. Not surprisingly, the Autograft group generally showed the best outcome. The SFI values, CAMP amplitude, CAMP latency, and histological analysis of the gastrocnemius in the Autograft group were all better than what we observed in the C/SAN group. However, the R/L ratio of footprint intensities and the G-ratio in the C/SAN group were close to those of the Autograft group. And encouragingly, the footprint intensities, CAMP amplitude, and the area of muscle fiber in the C/SAN-ER group were comparable to those of the Autograft group. The numbers of FG retrograde labeled motoneurons and

sensory neurons in the C/SAN and C/SAN-ER groups were markedly higher than those in the C/Hollow group, as was the number of myelinated axons in the regenerated nerves. Furthermore, the morphometric study of axonal regeneration revealed that the G-ratio and thickness of the myelin sheath in the C/SAN-ER group were close to those of the Autograft group.

Although SFI is widely used in the assessment of motor functional recovery after peripheral nerve injury, especially for the sciatic nerve, the results have been relatively unsatisfying (Navarro, 2016). Joint stiffness, abnormal paw placement, foot dragging, and autotomy make it difficult to measure the indexes (Dellon and Mackinnon, 1989). Moreover, SFI recovery after neurotmesis is minimal and discriminating between treatments for any type of repair is difficult. This is in stark contrast to the return to near normal values in the nerve-crush model (Dijkstra et al., 2000; Valero-Cabré and Navarro, 2002). Therefore, SFI analysis may cause bias. In this study, even in the Autograft group, the SFI was still not optimistic. Furthermore, the SFI did not differ significantly between the C/SAN and C/SAN-ER groups, although the thickness of the myelin sheath and the number of FG labeled motoneurons and sensory neurons indicated better outcomes in the C/SAN-ER group than in the C/SAN group. Additional measures should be tried to further increase the sensitivity of detection, such as individual footprint measures, toe angle, and the outward rotation of the hind feet (Navarro, 2016).

These findings indicated that axons could regenerate through the chitin conduits and reinnervate target muscles, and that greater regeneration and better functional recovery were observed when a small autogenous nerve was loaded into the conduit. Encouragingly, when the epineurium of the small nerve was removed, better recovery was achieved and some outcome indexes were close to what occurs with autogenous nerve grafts. The cauda equina nerve has been reported to have better permeability to chemicals due to the absence of epineurium (Sun et al., 2018). The small nerve we used in this study had a loose bundled structure that is similar to cauda equina nerve when the epineurium was exfoliated, which facilitated nutrient exchange and the secretion of neurotrophic factors. SCs play a critical role in peripheral nerve repair process. These cells dedifferentiate to a progenitor-like cell after injury, clear myelin debris, secret neurotrophic factors, and provide axon guidance cues (Jessen et al., 2015; Clements et al., 2017). Attempts have been made to enhance SC proliferation and migration (Yu et al., 2012; Chang et al., 2014; Motta et al., 2019). The small nerve inside the conduit contained a large number of SCs. The removal of the epineurium may facilitate the migration of SCs to the space between the wall of the conduit and the small nerve. Taken together, removing the epineurium could help the small nerve play a role in guiding the growth of the regenerating nerve.

Small autogenous nerves can be taken from a wide range of places in the body and are not limited in size. Thus, constructing a nerve graft that combines a chitin conduit with a small nerve is relatively easy, making it attractive to nerve surgeons. However, one limitation of this study lies in the location of the small nerve located within the conduit. In this study it was located eccentrically within the conduit, which might have made it less effective. To overcome this, we are considering physically fixing the small nerve in the center of the tube or improving the structure of the conduit in future studies. We are also planning to test this method when adding certain factors, like nerve growth factor or platelet-rich plasma in the space between the small nerve and the conduit to promote nerve regeneration. Furthermore, the size of the small autogenous nerve may have an important effect on the outcome. Varying diameters of the small nerves were not used in this study, but should be examined in the future.

In summary, a nerve graft composed of a chitin conduit and a small autogenous nerve can significantly improve the regeneration of nerves with defects. The conduit provided an optimal microenvironment for nerve regeneration, which was enhanced by including the small autogenous nerve inside. When the epineurium of the small autogenous nerve was removed, the nerve repair achieved a better outcome. Electrophysiological assessment, gastrocnemius histological analyses, and morphometric analysis of axonal regeneration showed that the nerve repair in this case was close to that of autogenous nerve transplantation. Therefore, a hybrid scaffold based on an autologous small nerve combined with a classical artificial biomaterial represents a new design for supporting peripheral nerve regeneration.

Additional files:
Additional Figure 1: Nerve gap bridged by different types of nerve grafts.
Additional Figure 2: Water penetration test.

References

Carvalho CR, López-Cebral R, Silva-Correia J, Silva JM, Mano JF, Silva TH, Freier T, Reis RL, Oliveira JM (2017) Investigation of cell adhesion in chitosan membranes for peripheral nerve regeneration. Mater Sci Eng C Mater Biol Appl 71:1122-1134.

Casal D, Mota-Silva E, Iria I, Alves S, Farinho A, Pen C, Lourenço-Silva N, Mascarenhas-Lemos L, Silva-Ferreira J, Ferraz-Oliveira M, Vassilenko V, Videira PA, Goyri-O'Neill J, Pais D (2018) Reconstruction of a 10-mm-long median nerve gap in an ischemic environment using autologous conduits with different patterns of blood supply: A comparative study in the rat. PLoS One 13:e0195692.

Chang HM, Liu CH, Hsu WM, Chen LY, Wang HP, Wu TH, Chen KY, Ho WH, Liao WC (2014) Proliferative effects of melatonin on Schwann cells: implication for nerve regeneration following peripheral nerve injury. J Pineal Res 56:322-332.

Clements MP, Byrne E, Camarillo Guerrero LF, Cattin AL, Zakka L, Ashraf A, Burden JJ, Khadayate S, Lloyd AC, Marguerat S, Parrinello S (2017) The wound microenvironment reprograms schwann cells to invasive mesenchymal-like cells to drive peripheral nerve regeneration. Neuron 96:98-114.e7.

Cui FZ, Ge J (2007) New observations of the hierarchical structure of human enamel, from nanoscale to microscale. J Tissue Eng Regen Med 1:185-191.

Cunha C, Panseri S, Antonini S (2011) Emerging nanotechnology approaches in tissue engineering for peripheral nerve regeneration. Nanomedicine 7:50-59.

Daly W, Yao L, Zeugolis D, Windebank A, Pandit A (2012) A biomaterials approach to peripheral nerve regeneration: bridging the peripheral nerve gap and enhancing functional recovery. J R Soc Interface 9:202-221.

Das S, Sharma M, Saharia D, Sarma KK, Sarma MG, Borthakur BB, Bora U (2015) In vivo studies of silk based gold nano-composite conduits for functional peripheral nerve regeneration. Biomaterials 62:66-75.

Dellon AL, Mackinnon SE (1989) Sciatic nerve regeneration in the rat. Validity of walking track assessment in the presence of chronic contractures. Microsurgery 10:220-225.

Dijkstra JR, Meek MF, Robinson PH, Gramsbergen A (2000) Methods to evaluate functional nerve recovery in adult rats: walking track analysis, video analysis and the withdrawal reflex. J Neurosci Methods 96:89-96.

Du J, Liu J, Yao S, Mao H, Peng J, Sun X, Cao Z, Yang Y, Xiao B, Wang Y, Tang P, Wang X (2017) Prompt peripheral nerve regeneration induced by a hierarchically aligned fibrin nanofiber hydrogel. Acta Biomater 55:296-309.

Firouzi MS, Firouzi M, Nabian MH, Zanjani LO, Zadegan SA, Kamrani RS, Rahimi-Movaghar V (2015) The effects of picric acid (2,4,6-trinitrophenol) and a bite-deterrent chemical (denatonium benzoate) on autotomy in rats after peripheral nerve lesion. Lab Anim (NY) 44:141-145.

Georgiou M, Golding JP, Loughlin AJ, Kingham PJ, Phillips JB (2015) Engineered neural tissue with aligned, differentiated adipose-derived stem cells promotes peripheral nerve regeneration across a critical sized defect in rat sciatic nerve. Biomaterials 37:242-251.

Gu X, Ding F, Williams DF (2014a) Neural tissue engineering options for peripheral nerve regeneration. Biomaterials 35:6143-6156.

Gu X, Ding F, Yang Y, Liu J (2011) Construction of tissue engineered nerve grafts and their application in peripheral nerve regeneration. Prog Neurobiol 93:204-230.

Gu Y, Zhu J, Xue C, Li Z, Ding F, Yang Y, Gu X (2014b) Chitosan/silk fibroin-based, Schwann cell-derived extracellular matrix-modified scaffolds for bridging rat sciatic nerve gaps. Biomaterials 35:2253-2263.

Jessen KR, Mirsky R, Lloyd AC (2015) Schwann cells: development and role in nerve repair. Cold Spring Harb Perspect Biol 7:a020487.

Jiang B, Zhang P, Zhang D, Fu Z, Yin X, Zhang H (2006) Study on small gap sleeve bridging peripheral nerve injury. Artif Cells Blood Substit Immobil Biotechnol 34:55-74.

Jiang X, Lim SH, Mao HQ, Chew SY (2010) Current applications and future perspectives of artificial nerve conduits. Exp Neurol 223:86-101.

Kehoe S, Zhang XF, Boyd D (2012) FDA approved guidance conduits and wraps for peripheral nerve injury: a review of materials and efficacy. Injury 43:553-572.

Kovacic U, Sketelj J, Bajrović FF (2003) Sex-related difference in collateral sprouting of nociceptive axons after peripheral nerve injury in the rat. Exp Neurol 184:479-488.

Li H, Cao M, Ma X, Zhang Y, Jin X, Liu K, Jiang L (2016) "Plug-and-Go"-type liquid diode: integrated mesh with janus superwetting properties. Adv Mater Interfaces 3:1600276.

Lu J, Sun X, Yin H, Shen X, Yang S, Wang Y, Jiang W, Sun Y, Zhao L, Sun X, Lu S, Mikos AG, Peng J, Wang X (2018) A neurotrophic peptide-functionalized self-assembling peptide nanofiber hydrogel enhances rat sciatic nerve regeneration. Nano Res 11:4599-4613.

Madduri S, Papaloizos M, Gander B (2010) Trophically and topographically functionalized silk fibroin nerve conduits for guided peripheral nerve regeneration. Biomaterials 31:2323-2334.

Maggipinto MJ, Ford J, Le KH, Tutolo JW, Furusho M, Wizeman JW, Bansal R, Barbarese E (2017) Conditional knockout of TOG results in CNS hypomyelination. Glia 65:489-501.

Melcangi RC, Giatti S, Calabrese D, Pesaresi M, Cermenati G, Mitro N, Viviani B, Garcia-Segura LM, Caruso D (2014) Levels and actions of progesterone and its metabolites in the nervous system during physiological and pathological conditions. Prog Neurobiol 113:56-69.

Meyer C, Stenberg L, Gonzalez-Perez F, Wrobel S, Ronchi G, Udina E, Suganuma S, Geuna S, Navarro X, Dahlin LB, Grothe C, Haastert-Talini K (2016) Chitosan-film enhanced chitosan nerve guides for long-distance regeneration of peripheral nerves. Biomaterials 76:33-51.

Motta CMM, Endres KJ, Wesdemiotis C, Willits RK, Becker ML (2019) Enhancing Schwann cell migration using concentration gradients of laminin-derived peptides. Biomaterials 218:119335.

Navarro X (2016) Functional evaluation of peripheral nerve regeneration and target reinnervation in animal models: a critical overview. Eur J Neurosci 43:271-286.

Noble J, Munro CA, Prasad VS, Midha R (1998) Analysis of upper and lower extremity peripheral nerve injuries in a population of patients with multiple injuries. J Trauma 45:116-122.

Pabari A, Yang SY, Mosahebi A, Seifalian AM (2011) Recent advances in artificial nerve conduit design: strategies for the delivery of luminal fillers. J Control Release 156:2-10.

Pan D, Mackinnon SE, Wood MD (2020) Advances in the repair of segmental nerve injuries and trends in reconstruction. Muscle Nerve 61:726-739.

Rao F, Yuan Z, Li M, Yu F, Fang X, Jiang B, Wen Y, Zhang P (2019) Expanded 3D nanofibre sponge scaffolds by gas-foaming technique enhance peripheral nerve regeneration. Artif Cells Nanomed Biotechnol 47:491-500.

Rao F, Wang Y, Zhang D, Lu C, Cao Z, Sui J, Wu M, Zhang Y, Pi W, Wang B, Kou Y, Wang X, Zhang P, Jiang B (2020) Aligned chitosan nanofiber hydrogel grafted with peptides mimicking bioactive brain-derived neurotrophic factor and vascular endothelial growth factor repair long-distance sciatic nerve defects in rats. Theranostics 10:1590-1603.

Ray WZ, Mackinnon SE (2010) Management of nerve gaps: autografts, allografts, nerve transfers, and end-to-side neurorrhaphy. Exp Neurol 223:77-85.

Robinson LR (2000) Traumatic injury to peripheral nerves. Muscle Nerve 23:863-873.

Seddon HJ, Medawar PB, Smith H (1943) Rate of regeneration of peripheral nerves in man. J Physiol 102:191-215.

Sun X, Wang Y, Guo Z, Xiao B, Sun Z, Yin H, Meng H, Sui X, Zhao Q, Guo Q, Wang A, Xu W, Liu S, Li Y, Lu S, Peng J (2018) Acellular cauda equina allograft as main material combined with biodegradable chitin conduit for regeneration of long-distance sciatic nerve defect in rats. Adv Healthc Mater 7:e1800276.

Tang P, Whiteman DR, Voigt C, Miller MC, Kim H (2019) No difference in outcomes detected between decellular nerve allograft and cable autograft in rat sciatic nerve defects. J Bone Joint Surg Am 101:e42.

Tos P, Ronchi G, Papalia I, Sallen V, Legagneux J, Geuna S, Giacobini-Robecchi MG (2009) Chapter 4: Methods and protocols in peripheral nerve regeneration experimental research: part I-experimental models. Int Rev Neurobiol 87:47-79.

Valero-Cabré A, Navarro X (2002) Functional impact of axonal misdirection after peripheral nerve injuries followed by graft or tube repair. J Neurotrauma 19:1475-1485.

Wang B, Li P, Shangguan L, Ma J, Mao K, Zhang Q, Wang Y, Liu Z, Mao K (2018) A novel bacterial cellulose membrane immobilized with human umbilical cord mesenchymal stem cells-derived exosome prevents epidural fibrosis. Int J Nanomedicine 13:5257-5273.

Wang L, Lu C, Yang S, Sun P, Wang Y, Guan Y, Liu S, Cheng D, Meng H, Wang Q, He J, Hou H, Li H, Lu W, Zhao Y, Wang J, Zhu Y, Li Y, Luo D, Li T, et al. (2020) A fully biodegradable and self-electrified device for neuroregenerative medicine. Sci Adv 6:eabc6686.

Wang X, Hu W, Cao Y, Yao J, Wu J, Gu X (2005) Dog sciatic nerve regeneration across a 30-mm defect bridged by a chitosan/PGA artificial nerve graft. Brain 128:1897-1910.

Xue F, Wu EJ, Zhang PX, Li-Ya A, Kou YH, Yin XF, Han N (2015) Biodegradable chitin conduit tubulation combined with bone marrow mesenchymal stem cell transplantation for treatment of spinal cord injury by reducing glial scar and cavity formation. Neural Regen Res 10:104-111.

Yu B, Zhou S, Wang Y, Qian T, Ding G, Ding F, Gu X (2012) miR-221 and miR-222 promote Schwann cell proliferation and migration by targeting LASS2 after sciatic nerve injury. J Cell Sci 125:2675-2683.

Yuan YS, Niu SP, Yu F, Zhang YJ, Han N, Lu H, Yin XF, Xu HL, Kou YH (2020) Intraoperative single administration of neutrophil peptide 1 accelerates the early functional recovery of peripheral nerves after crush injury. Neural Regen Res 15:2108-2115.

Zhang P, Yin X, Kou Y, Han N, Wang T, Tian G, Lu L, Jiang B (2015) Peripheral nerve mutilation through biodegradable conduit small gap tubulisation: a multicentre randomised trial. Lancet 386:S40.

Zhang PX, Li J, Han N, Zhang HB, Zhao GQ, Jiang BG (2008) Effect of nerve fragments and nerve growth factor on biological conduit small gap bridging to repair peripheral nerve injury. Zhongguo Zuzhi Gongcheng Yanjiu yu Linchuang Kangfu 12:4465-4468.

Zhu S, Ge J, Wang Y, Qi F, Ma T, Wang M, Yang Y, Liu Z, Huang J, Luo Z (2014) A synthetic oxygen carrier-olfactory ensheathing cell composition system for the promotion of sciatic nerve regeneration. Biomaterials 35:1450-1461.
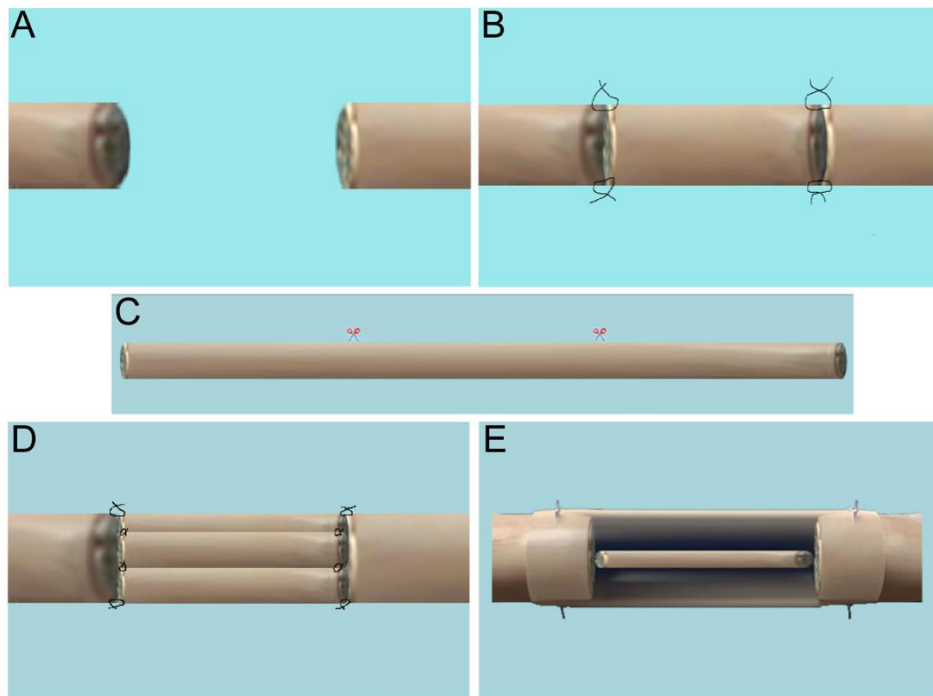
Additional Figure 1 Nerve gap bridged by different types of nerve grafts.

(A) Nerve defect. (B) Nerve defect repaired with an autologous nerve graft. (C, D) Nerve defect repaired with the cable-style nerve graft made of small nerves. (E) Nerve defect repaired with a chitin scaffold incorporating a single small autologous nerve with fewer fibers.
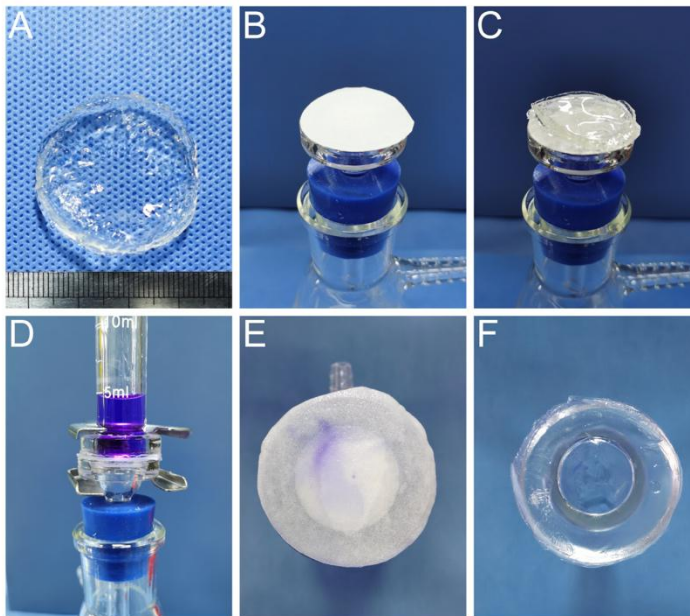
Additional Figure 2 Water penetration test.

(A) The chitin membrane. (B, C) A filter paper was stacked underneath the membrane. (D) The filter paper and the chitin membrane were sandwiched between two glass tubes, and 5 ml crystal violet solution was added to the glass tube above. (E) The filter paper under the membrane was dyed purple. (F) The chitin membrane remained intact without damage.